
Aerosol Science and Technology
Publication details, including instructions for authors and subscription information:
http://www.tandfonline.com/loi/uast20

# Characterization of a Vortex Shaking Method for Aerosolizing Fibers

Bon Ki Ku [a] , Gregory Deye [a] & Leonid A. Turkevich [a]
[a] Centers for Disease Control and Prevention , National Institute for Occupational Safety and Health , Cincinnati , Ohio , USA
Accepted author version posted online: 27 Aug 2013.

To cite this article: Bon Ki Ku , Gregory Deye & Leonid A. Turkevich (2013) Characterization of a Vortex Shaking Method for Aerosolizing Fibers, Aerosol Science and Technology, 47:12, 1293-1301, DOI: 10.1080/02786826.2013.836588

To link to this article: http://dx.doi.org/10.1080/02786826.2013.836588

*Aerosol Science and Technology*, 47:1293–1301, 2013
ISSN: 0278-6826 print / 1521-7388 online
DOI: 10.1080/02786826.2013.836588

# Characterization of a Vortex Shaking Method for Aerosolizing Fibers

**Bon Ki Ku, Gregory Deye, and Leonid A. Turkevich**
*Centers for Disease Control and Prevention, National Institute for Occupational Safety and Health, Cincinnati, Ohio, USA*



**Generation of well-dispersed, well-characterized fibers is important in toxicology studies. A vortex-tube shaking method is investigated using glass fibers to characterize the generated aerosol. Controlling parameters that were studied included initial batch amounts of glass fibers, preparation of the powder (e.g., preshaking), humidity, and airflow rate. Total fiber number concentrations and aerodynamic size distributions were typically measured. The aerosol concentration is only stable for short times ($t < 10$ min) and then falls precipitously, with concomitant changes in the aerosol aerodynamic size distribution; the plateau concentration and its duration both increase with batch size. Preshaking enhances the initial aerosol concentration and enables the aerosolization of longer fibers. Higher humidity strongly affects the particle size distribution and the number concentration, resulting in a smaller modal diameter and a higher number concentration. Running the vortex shaker at higher flow rates ($Q > 0.3$ lpm), yields an aerosol with a particle size distribution representative of the batch powder; running the vortex shaker at a lower aerosol flow rate ($Q \sim 0.1$ lpm) only aerosolizes the shorter fibers. These results have implications for the use of the vortex shaker as a standard aerosol generator.**

Received 2 May 2013; accepted 19 July 2013.
This article not subject to United States copyright law.

Disclaimer: The findings and conclusions in this report are those of the authors and do not necessarily represent the views of the National Institute for Occupational Safety and Health. Mention of product or company name does not constitute endorsement by the Centers for Disease Control and Prevention.

None of the authors has a financial relationship with a commercial entity that has an interest in the subject of this manuscript.

The authors thank Mariko Ono-Ogasawara (Japan National Institute of Occupational Safety and Health, and Japan Fibrous Material Research Association, JFMRA) for the samples of the GW1 glass fibers used in this study. We thank Elizabeth Ashley (University of Cincinnati), for assisting in the analysis of PCM images of the fibers. We thank Doug Evans and Liming Lo for helpful discussions. This work was funded by the NORA program at NIOSH.

Address correspondence to Bon Ki Ku, Centers for Disease Control and Prevention (CDC), National Institute for Occupational Safety and Health (NIOSH), 4676 Columbia Parkway, MS-R3, Cincinnati, OH 45226, USA. E-mail: bik5@cdc.gov

## 1. INTRODUCTION

Generation of well-dispersed, well-characterized fibers is important in toxicology studies. Historically, aerosols of asbestos and man-made vitreous fibers were extensively investigated. During the past decade, airborne fibrous carbonaceous nanoparticles, such as carbon nanotubes (CNTs) and carbon nanofibers (CNFs), have received scrutiny owing to their morphological similarity with asbestos. Concerns as to their potential toxicity derive from their thin fiber-like structure and their insolubility in the lungs, attributes common with harmful asbestos fibers (Poland et al. 2008; Donaldson and Poland 2009; Kisin et al. 2011). Various approaches to generating fibrous aerosol particles from bulk powder materials have been used for toxicology tests (Ku et al. 2006; Baron et al. 2008; McKinney et al. 2009; Kim et al. 2010).

Spurny (1980) reviewed the earlier aerosolization methods such as pulverizing fibrous materials and fluidized-bed aerosol generation, focusing on mineral fibers. Maynard et al. (2004), in order to simulate exposures encountered in the field, used a vortex generator to aerosolize CNT particles so as to monitor these aerosols in the lab. Ku et al. (2006) agitated CNF powder using a vortex shaker in order to study the CNF aerosol. Baron et al. (2008) developed an aerosol generator for extremely low-density single-walled carbon nanotubes (SWCNTs) for inhalation studies, using an acoustic feeder and a knife mill. McKinney et al. (2009) generated a respirable fraction of multi-walled carbon nanotubes (MWCNTs) from bulk material using a similar acoustic feeder. Ku and Kulkarni (2009) dispersed SWCNTs using an electrospray of a SWCNT suspension to get less agglomerated SWCNT aerosol particles. Kim et al. (2010) used a similar electrospray method to deliver airborne nanoparticles such as $TiO_2$ and CNT for *in vitro* and *in vivo* studies. Recently, Ku et al. (2013) used the vortex shaker to aerosolize glass fibers to study the efficacy of screens to alter the fiber length distribution within the aerosol. In all of these studies, the common aim was to better disperse the material so as to obtain deagglomerated particles in the aerosol.

Current fiber measurement techniques arose primarily due to health concerns over asbestos exposure. Whether to provide

samples for *in vitro* testing (Zeidler-Erdely et al. 2006) or to generate aerosols for inhalation studies, the aerosolization method needs to successfully aerosolize fibers without undue agglomeration. Vortex shaking has been used to aerosolize fibrous particles such as CNFs and CNTs because of its simplicity and ease of use (Ku et al. 2006; Maynard et al. 2007). It is believed that vortex shaking imparts additional mechanical energy to break up agglomerates entangled in the powder, compared to other less aggressive methods such as acoustic generators. The vortex shaking method is currently under discussion by the International Standards Organization as a candidate ISO technical specification to evaluate nanoparticle release from powders (Ogura et al. 2009; ISO 2012).

In this study, we conducted a series of experiments to characterize a vortex-tube shaking method of generating aerosols of fibrous particles. We investigated a variety of controlling parameters (initial batch amounts of glass fibers, preshaking of the powder, humidity, and aerosol flow rates) on the characteristics of the aerosolized fibers. Total fiber number concentration and aerodynamic size distributions were measured. Particular attention was paid to temporal changes (i.e., decay) of the aerosols as these controlling parameters were varied.

## 2. MATERIALS

Glass fiber powder (GW1), supplied by the Japan Fibrous Material Research Association (JFMRA) (Kohyama et al. 1997), was aerosolized by the vortex shaker for this study. The glass fibers in this sample have a nominal geometric mean length, $L_{\text{geom}} \sim 20.0$ $\mu$m (50% cut-off length $L_{50} \sim 20.0$ $\mu$m), with geometric standard deviation, GSD $\sim 2.58$, and a nominal geometric mean diameter, $d_{\text{geom}} \sim 0.88$ $\mu$m, with GSD $\sim 3.10$ (Kohyama et al. 1997). In the current study, we found slightly lower $L_{\text{geom}} \sim 18$ $\mu$m and $L_{50} \sim 15$ $\mu$m, than those reported by Kohyama and colleagues (see the result and discussion section). This same material was used in our previous studies (Ku et al. 2012, 2013), where aerosols of glass fibers were generated by the vortex shaking method.

For the initial phase of this study, a weighed amount of the glass fibers was loaded into the vortex shaker tube "as received." We also investigated aerosolization of powder which had been "pre-shaken"—namely, the vortex shaker was run so that the vortex tube underwent its usual rotational motion but where no air flow was introduced so as to carry away the dust cloud. For our long-duration study, we periodically interrupted the vortex shaking in order to sieve the powder remaining at the bottom of the vortex shaker tube. Sieving of remnant fibers was performed using a 35-mesh stainless steel sieve (i.e., aperture size $= 425$ $\mu$m).

## 3. EXPERIMENTAL METHODS

The experimental setup is shown in Figure 1. A vortex shaker (Vortex-Genie 2, Scientific Industries, Inc.) is operated at variable speeds of 600–3200 rpm, executing a large ($r = 6$ mm) orbit for aggressive vortex shaking; we typically operated the vortex shaker at 70% maximum rotation speed. A batch of glass fiber powder is placed at the bottom of a Pyrex tube (depth $h =$ 20 cm, diameter OD $= 2.5$ cm), which is anchored by means of a pop-off cup on top of the vortex shaker (Figure 1).

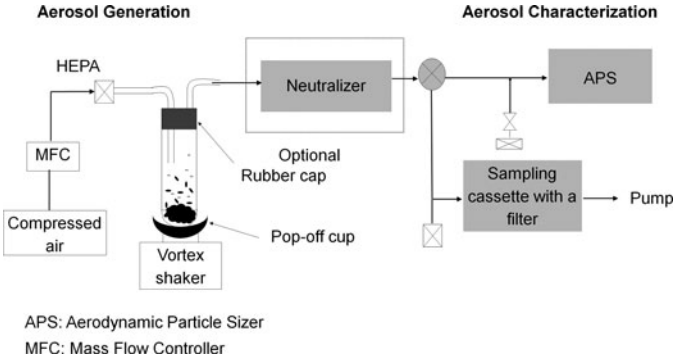


FIG. 1. Experimental setup.

HEPA filtered air is provided into the top of the vortex tube, and the aerosol is similarly drawn from a second port at the top of the vortex tube which is sealed with a rubber cap; the air flow is presumably directed downward along one side of the tube and upward along the opposite side. The Reynolds number of the flow within the vortex tube is estimated to be Re $\sim 10^1$–$10^2$, so the airflow should be laminar. In order to test the effect of humidity, a bubbler was used to saturate the incoming air stream to 90% relative humidity (RH) which was measured by a thermo-hygrometer (Digi-Sense®, Cole-Parmer). When in operation, the base of the vortex tube executes rotary motion by the vortex shaker; the powder at the base of the tube is sufficiently mechanically agitated to loft a cloud of fibers in the tube. The overall airflow sweeps the lofted particles out as an aerosol. The unit may also be operated in the absence of an airflow (preshaking mode). In this closed mode, the cloud is in dynamic equilibrium with the powder: the powder is mechanically agitated, transferring material to the dust cloud, but material also falls from the dust cloud back onto the powder pile.

Aerodynamic size distributions of the airborne glass fibers from the vortex shaker were measured by sampling the aerosol through an Aerodynamic Particle Sizer (3321, TSI Inc., Shoreview, MN, USA). Aerodynamic size distributions of generated glass fibers were measured as a function of time, and decay of total number concentration with time for different initial batch amounts was measured continuously by APS for two to three hours. APS measurement was made at an aerosol flow rate of 1.5 lpm. Total fiber number concentrations were obtained using the APS and integrating over all channels.

Physical length distributions were measured by sampling the airborne fibers through a mixed cellulose ester (MCE) filter (SKC Inc., Eighty Four, PA, USA), mounted in a 25 mm conductive cassette (#225-321A, SKC Inc.). The MCE filters were acetone clarified, and representative fibers were imaged by a

phase contrast microscope (PCM) with 40X objective magnification; lengths were measured using Motic software (Motic Incorporation Ltd., Hong Kong), and length distributions were constructed, as discussed previously (Ku et al. 2013).

### 3.1. Control Parameters

In order to investigate aerosol generation characteristics of the vortex shaker, we considered four control parameters: initial batch amounts of glass fibers, powder preparation (i.e., preshaking), humidity, and rate of the airflow.

- Initial batch amount: 0.1, 0.2, 0.5, 0.8, and 1.0 g;
- Powder preparation:
  (a) No preshaking (powder 'as received'),
  (b) 30 min preshaking (running the rotating vortex generator but without airflow);
- Humidity:
  (a) Dry air (about 5–10%),
  (b) RH = 90%;
- Rate of airflow: 0.1, 0.3, 0.9, 1.5, 2.5 lpm.

To ensure the effect of each control parameter on the aerosol characteristics such as size distributions, at least two to three tests were conducted under the same experimental condition.

## 4. RESULTS AND DISCUSSION

In the results discussed below, we find that the aerosol of glass fibers generated by the vortex shaker depends on a variety of control parameters (batch size, powder preparation, humidity, airflow rate) and is not stable over long run times. Thus, while the vortex generator is low cost, easy to set up and use, great care should be exercised in comparing aerosols generated in this manner from different labs, or even at different times within the same lab using the same equipment.

### 4.1. Time Dependence of the Aerosol Concentration as a Function of Batch Size

Figure 2 shows the time evolution of the total number concentration of glass fibers generated by the vortex shaker for various batch amounts of fiber powder at an airflow rate $Q = 1.5$ lpm. The number concentration is stable for the first 5–10 min and then drops precipitously. The initial total number concentration plateau increases with initial batch size; the time duration of the initial plateau concentration also seems to increase with batch size.

Following an initial phase of stable operation, the aerosol concentration is always found to decay. This decay is qualitatively similar for all batches, although the details of the time-dependence seem to be batch dependent, with the smaller batches decaying more gradually than the larger batches. For the $M_i = 0.1$ g batch, the initial time decay is $\sim t^{-3/4}$, which crosses over to $\sim t^{-2}$ at the later times; for the $M_i = 0.2$ g batch, the time decay is $\sim t^{-3/2}$; for the larger batches ($M_i > 0.5$ g), the time decay is $\sim t^{-2}$. For the $M_i = 0.3$ g batch material (shown in the inset), the strength of the vortex shaking was repeatedly adjusted, with the aim of stabilizing the aerosol concentration; with this manual feedback, the number concentration could be stabilized for about 40 min.

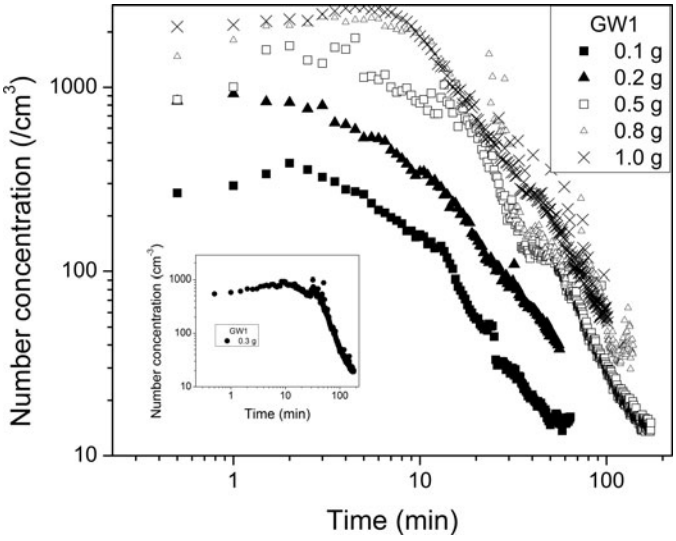


FIG. 2. Total fiber number concentration of glass fibers generated by vortex shaker as a function of time for various initial batch amounts. Inset: total fiber number concentration ($M_i = 0.3$ g) where vortex shaker conditions are altered to prolong initial fiber concentration.

### 4.2. Time Dependence of Size Distributions as a Function of Batch Size

Figure 3a shows the time evolution of the aerodynamic size distribution of glass fibers generated by vortex shaker (without preshaking) for the smaller batch amount, $M_i = 0.2$ g, again at airflow rate $Q = 1.5$ lpm. The distribution is essentially unimodal, with a tail to larger aerodynamic diameters. Aerodynamically larger fibers ($d_{ae} > 2$ $\mu$m) are quickly depleted from the aerosol stream, relative to the aerodynamically smaller fibers. Fibers from a larger initial batch, $M_i = 1.0$ g, under the same airflow conditions ($Q = 1.5$ lpm) show one mode initially and later two modes (Figure 3b). The decay of the primary mode ($d_{ae} \sim 1$ $\mu$m) seems to be similar to that for the smaller batch amount (0.2 g).

Figure 4 is a more detailed plot of the aerodynamic size distribution for this base case—initial batch size $M_i = 0.2$ g, dry air, airflow rate $Q = 1.5$ lpm, and no preshaking—over the shorter time period $0 < t < 10$ min; note, that this is within the "plateau" region, as indicated by the total number concentration. Even within the plateau region, the peaks in the aerodynamic diameter distribution decay by a factor of 2 over 10 min, although the overall shape of the entire aerodynamic diameter distribution is relatively unchanged.

We examined the effects on aerosol quality by changing two parameters within this short initial time period: preshaking the fiber powder, and changing the humidity of the air passing through the vortex generator.

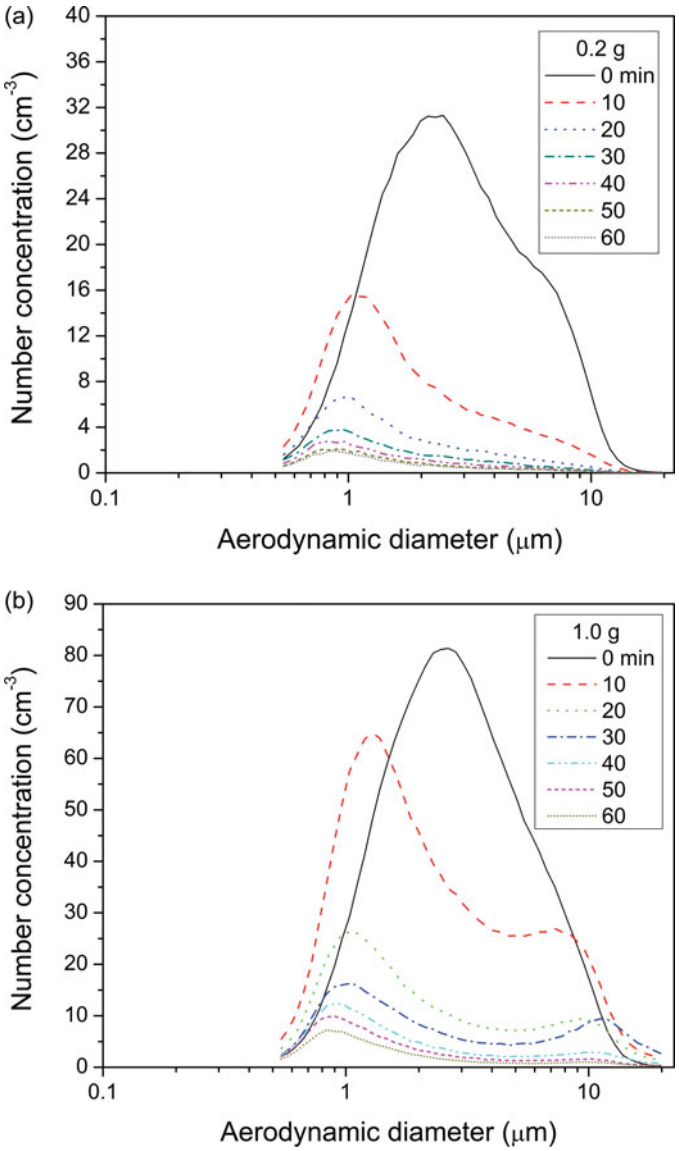


FIG. 3. Number size distribution of glass fibers generated without preshaking and measured by an aerodynamic particle sizer for different batch amounts. (a) Batch amount 0.2 g and (b) 1.0 g. Dry air and airflow rate $Q = 1.5$ lpm. (Color figure available online.)

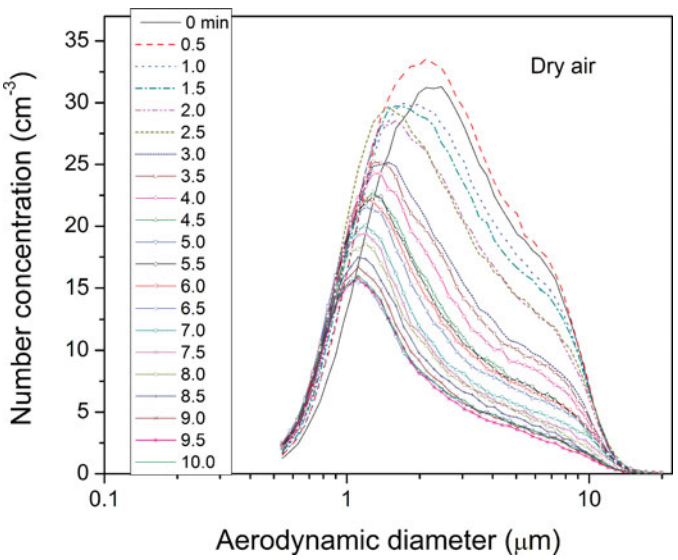


FIG. 4. Number size distribution of glass fibers generated without preshaking and measured by an aerodynamic particle sizer. Batch amount 0.2 g, dry air, and airflow rate $Q = 1.5$ lpm. (Color figure available online.)

### 4.3. Effect of Preshaking on Aerosol Generation

Figure 5a shows the time evolution of the aerodynamic size distribution of glass fibers generated by the vortex shaker in dry air for batch amount $M_i = 0.2$ g, again at airflow rate $Q = 1.5$ lpm, but where the initial powder was shaken for 30 min prior to aerosolization in the vortex-shaker (preshaking).

With preshaking, the initial concentration in the aerosol is essentially twice that of the control (no preshaking, shown in Figure 4). Also, preshaking aerosolizes more of the larger fibers (there is significantly more weight in the distribution at the larger aerodynamic diameters)—this is probably due to enhanced dispersion of the fibers by preshaking of the powder in the tube. Both distributions—unshaken (Figure 4) and preshaken (Figure 5a)—decay with time, and after ~3 min, they effectively coincide, removing all effect of whether or not the initial powder had been preshaken; at $Q \sim 1.5$ lpm, $t \sim 3$ min corresponds to ~100 exchange volumes through the vortex shaker tube. Since the initial aerosol of the preshaken powder contains more of the larger fibers than does the control, and since the two aerosol distributions coincide after 3 min of running the vortex shaker, the larger fibers are swept out more efficiently than the shorter fibers, once the airflow is established.

### 4.4. Effect of Humidity on Aerosol Generation

Raising the humidity from dry air to RH = 90% also changed the size distributions of fibers in the aerosol (Figure 5b); the modal diameter is shifted to a smaller size (from 1.0 $\mu$m to about 0.8 $\mu$m), and the maximum number concentration increased by a factor of 5. This concentration effect is not transient; even after 10 min, the maximum number concentration, which has decayed in both samples, is still higher in the humid sample, relative to the dry sample, by a factor of 7. The humidity dependence clearly must derive from the surface chemistry of the material being aerosolized (e.g., at high humidity, water may condense on the surface of glass fibers, whereas this would not be expected to happen with hydrophobic materials such as CNTs). The fiber size distribution is also altered by the humidity: after 1 min, under dry conditions, $N(d_{ae}{\sim}1\ \mu m)/N(d_{ae}{\sim}2\ \mu m) \sim 1.1$, whereas under RH = 90%, $N(d_{ae}{\sim}1\ \mu m)/N(d_{ae}{\sim}2\ \mu m) \sim 1.3$; after 10 min, under dry conditions, $N(d_{ae}{\sim}1\ \mu m)/N(d_{ae}{\sim}2\ \mu m) \sim 2$, whereas, under RH ~ 90%, $N(d_{ae}{\sim}1\ \mu m)/N(d_{ae}{\sim}2\ \mu m) \sim 5$. Again we see efficient temporal depletion of the larger fibers from the aerosol, which depletion is further enhanced by humidity.

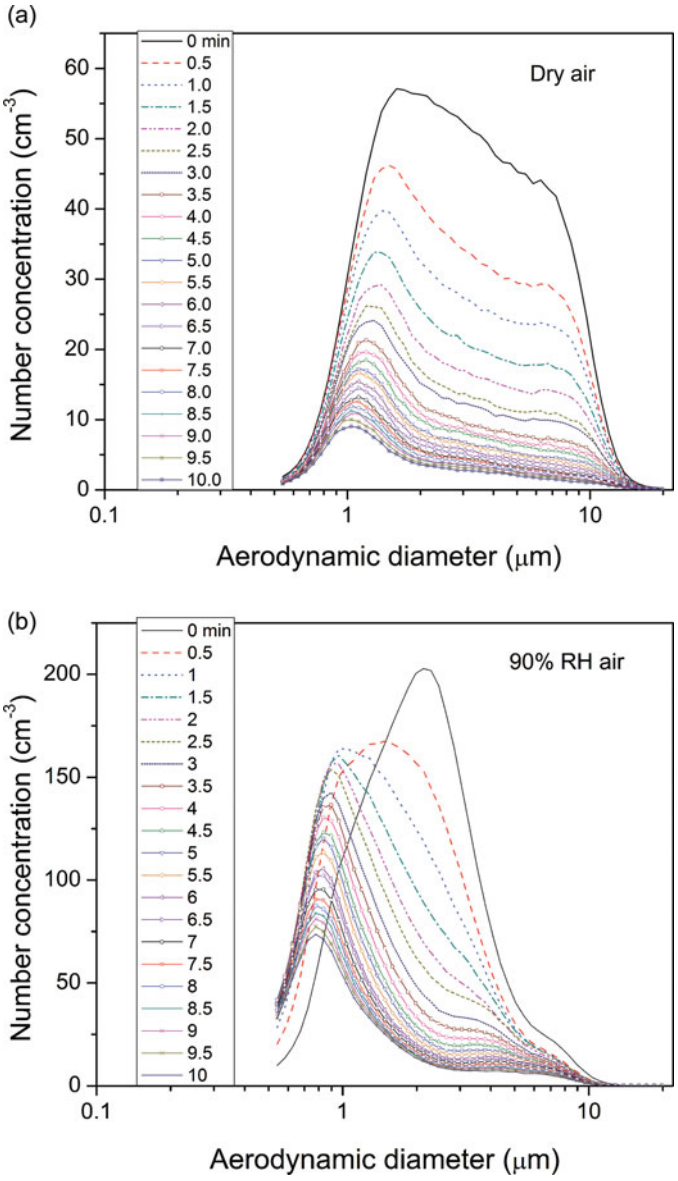


FIG. 5. Number size distribution of glass fibers generated by vortex shaker as a function of time for batch amount of 0.2 g after 30 min preshaking. (a) In dry air and (b) in humid air (RH = 90%). (Color figure available online.)

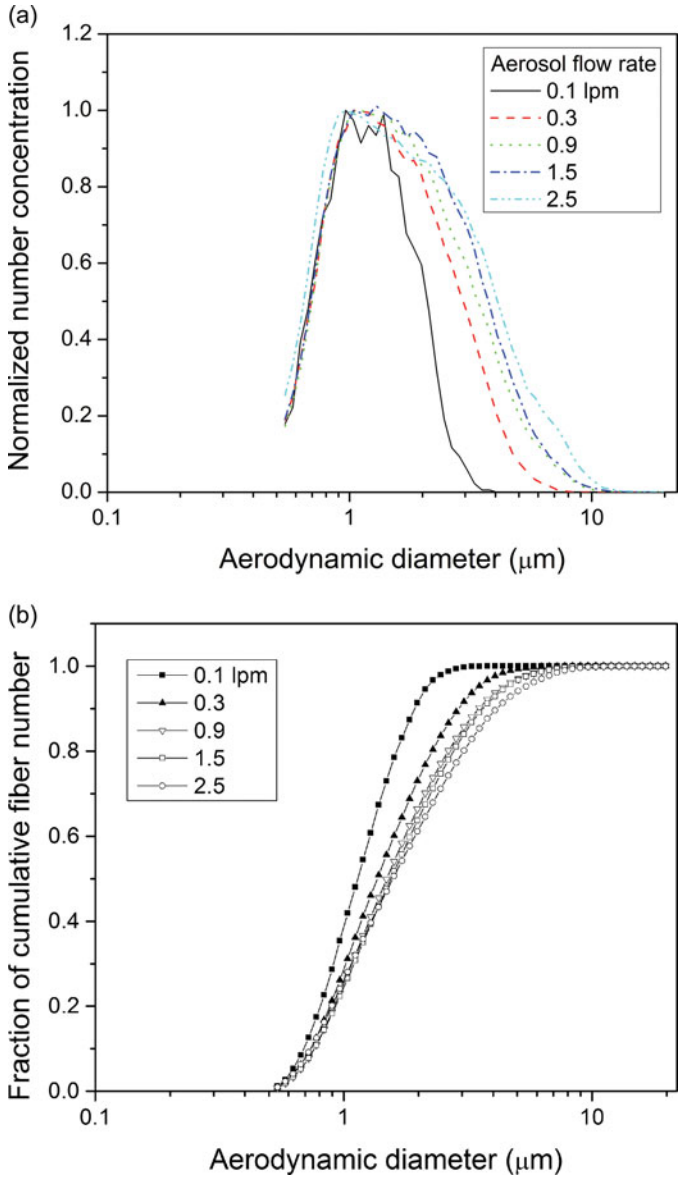


FIG. 6. Size distributions of glass fibers as a function of aerodynamic diameter for different aerosol flow rates (batch amount $M_i = 0.2$ g). (a) Size distribution normalized by peak value. (b) Fraction of cumulative fiber number. (Color figure available online.)

### 4.5. Effect of Airflow Rate on Aerosol Generation

We investigated the vortex shaking method at different aerosol flows. The aerodynamic size distribution at different aerosol flow rates (dry air) is shown in Figure 6a—the same data is plotted (Figure 6b) as a cumulative fiber number fraction. For fibers aerosolized at high aerosol flow rates, $Q > 0.9$ lpm, the aerodynamic size distributions are relatively unaffected by flow rate; however, at the lower flow rates, $Q < 0.9$ lpm, the aerodynamic size distribution becomes narrower as the aerosolizing flow rate is reduced. In particular, at the lowest flow rate, $Q =$ 0.1 lpm, the aerodynamic size distribution spanned only 4 $\mu$m; by contrast, at $Q \sim 1.5$ lpm, the aerodynamic size distribution spans 20 $\mu$m. It would appear that, at the lower flow rates, the larger fibers are not being aerosolized.

The flow rate dependence of the aerosol aerodynamic diameter distribution is confirmed by direct physical measurement of the lengths of fibers collected from the different aerosol streams. Figure 7 shows the cumulative fiber number fraction as a function of fiber length (measured by PCM) for the different aerosol flow rates.

At the lowest flow rate, $Q \sim 0.1$ lpm, only the shortest fibers are aerosolized by the vortex shaker; however, for $Q > 0.3$ lpm, the physical length distribution does not depend on flow rate and is representative of the physical length distribution of the

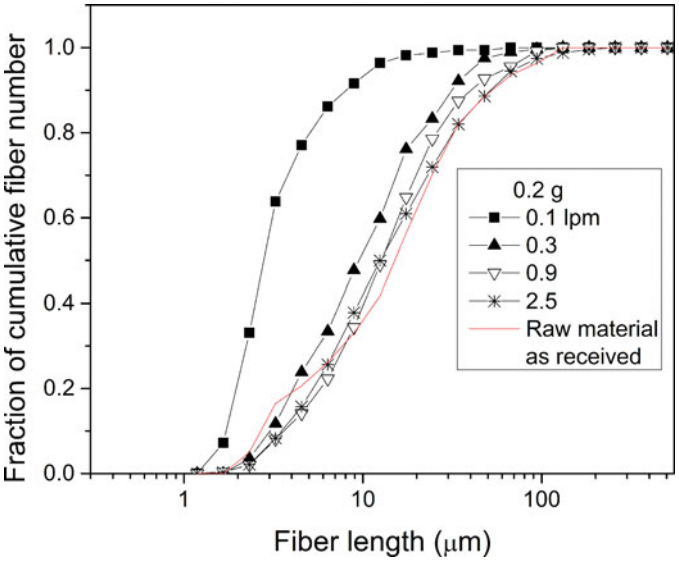


FIG. 7. Fraction of cumulative fiber number vs. fiber length for different aerosol flow rates. (Color figure available online.)

batch powder. Quantitatively, the 50% cut-off length depends on aerosol flow rates: $L_{50} \sim 10\ \mu$m, for $Q > 0.3$ lpm, is drastically reduced to $L_{50} \sim 2.7\ \mu$m, for $Q \sim 0.1$ lpm, indicating that running the vortex shaker at the lowest airflow rate preferentially aerosolizes shorter fibers.

### 4.6. Effects of Running the Vortex Shaker for Long Times

We have seen time-dependent effects on the aerosol number concentration (Figure 2), on a time scale of 2 h, and changes in the aerosol size distribution (Figures 4 and 5), on an even shorter time scale of 10 min. We also looked at very long time effects, on a time scale up to 18 h. Since the aerosol size distribution is changing, potential mechanisms need to be considered which might affect the preferential aerosolization of different length fractions as a function of time. Over time, size segregation may occur within the powder at the bottom of the vortex shaker tube via percolation and granular convection, with the smaller fibers settling through the interstices formed by the packing of the larger fibers (i.e., percolation) and by carrying particles down at the walls and up in the center of the tube (i.e., granular convection), the so-called "Brazil nut effect" (Rosato et al. 1987; Knight et al. 1993, 1996; Moebius et al. 2001; Jenkins and Yoon 2002); this would tend to reduce the aerosolization of the shorter fibers with time. Alternatively, when running at the lower flow rates, $Q \sim 0.1$ l pm, only the smaller fibers are aerosolized, so that, over time, the powder should be depleted of short fibers (i.e., "enriched" with long fibers). Again, we would expect to see a reduction in the aerosolization of the short fibers with time.

We thus examined the preferential separation of smaller fibers by running the vortex shaker at $Q \sim 0.1$ l pm (dry air) for long times (up to 18 h). Figure 8 shows the cumulative number fraction as a function of fiber length for different operating conditions of the vortex shaker: 7.5 h run, 10 h run with sieving, 18 h run, 18 h run with sieving, and 16 h run with sieving. The length distribution of the raw material is included in Figure 8 for comparison.

In this set of experiments, sieving of fibers remaining in the vortex tube was performed frequently (e.g., three to five times) after running the vortex shaker for several hours. Aggressive sieving of the residual fibers is motivated by the hypothesis that, during the operation of the vortex shaker, longer fibers might form entangled agglomerates (see Appendix), possibly immobilizing some of the residual smaller fibers. Aggressive sieving (where the material is pushed through the mesh) would tend to break up these agglomerates and liberate the smaller fibers for subsequent aerosolization in the vortex shaker.

We first discuss the long time behavior without sieving. The fiber length distribution of fibers collected from the aerosol stream after running the vortex shaker without sieving, for 7.5 and 18 h, is shown in Figure 8. There is minimal change in the aerosol after 7.5 h (i.e., the aerosol at 18 h looks very similar to the aerosol at 7.5 h); however, the long-time aerosol is depleted of short fibers, relative to the starting material. While the ($t = 0$) starting material has about 30% fibers smaller than 10 $\mu$m, running the vortex shaker for $t \sim 7.5$ (18) h yields about 18% (15%) fibers smaller than 10 $\mu$m; similarly, the 50% cut-off length is increased from $L_{50} \sim 18\ \mu$m ($t = 0$) to $L_{50} \sim 25\ \mu$m ($t \sim 7.5$ h) and $L_{50} \sim 28\ \mu$m ($t \sim 18$ h). This very long time ($t >$ h) depletion of the short fibers from the aerosol is opposite to the shorter time ($t \sim 10$ min) depletion of the long fibers from the aerosol.

We now discuss the long time behavior with periodic sieving. Figure 8 also shows data for two runs of the vortex shaker with

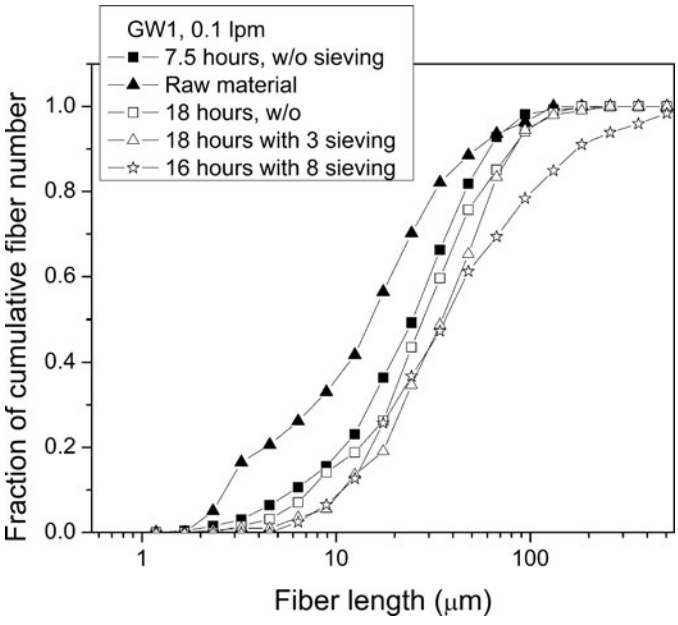


FIG. 8. Fraction of cumulative fiber number vs. fiber length for different operation conditions (16 and 18 h runs) of the vortex shaker at 0.1 lpm of aerosol flow rate.

aggressive sieving: 16 h (8 sievings) and 18 h (3 sievings). For both cases, the 50% cut-off lengths $L_{50} \sim 35$ $\mu$m. The length distributions coincide for shorter fiber lengths; the fractions of fibers smaller than 10 $\mu$m are about 9%, suppressed from 30% of the starting material. However, the length distributions are quite different for the longer fiber lengths; the case of 16 h (8 sievings) contains more of the long fibers than the case of 18 h (3 sievings). Since the run times are comparable, this suggests that increasing the number of sievings enriches the final aerosol in long fibers.

Figure 9 shows the total number concentrations as a function of time for 18 h (a) without and (b) with sieving. For the case with no sieving (Figure 9a), the aerosol concentration is well-behaved, decreasing with a decay time $\tau \sim 3$ h. The case with sieving (Figure 9b) is more complicated and not at all understood. There is an initial increase (over 200 min) in concentration (prior to any sieving event), and then a gradual decrease in concentration, much slower than in the no sieving case; also the sieving process seems to generate concentration spikes in the aerosol, which decay very quickly.

Figure 10 show the corresponding aerodynamic diameter distributions (a) without and (b) with sieving. In the case without sieving, there is a short time ($t < 60$ min) shift in the aerodynamic diameter distribution to the mode at about 0.8–1.0 $\mu$m, which is subsequently stable. When the vortex shaking is periodically interrupted with sieving, the aerodynamic diameter distribution retains weight at a higher mode ($d_{ae} \sim 1.6$ $\mu$m) for the duration of the run. Also the initial (unexplained) increase in concentration is accompanied by changes in the initial aerodynamic diameter distribution.

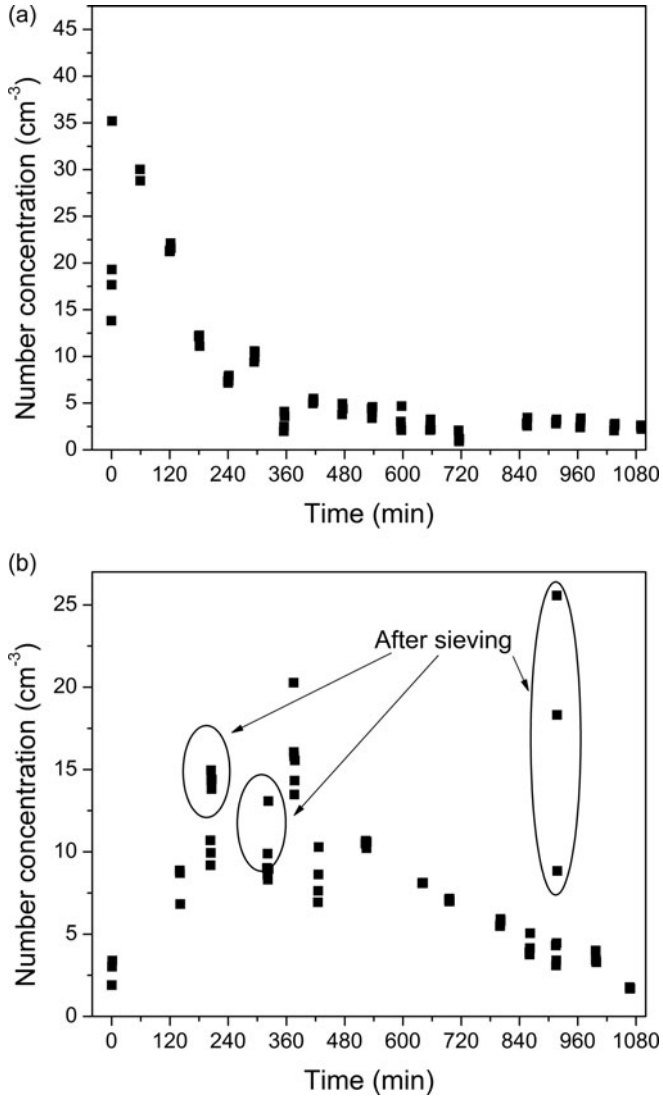


FIG. 9. Total number concentration measured at different times during the 18 h run at 0.1 lpm of aerosol flow rate. (a) Without sieving and (b) with sieving.

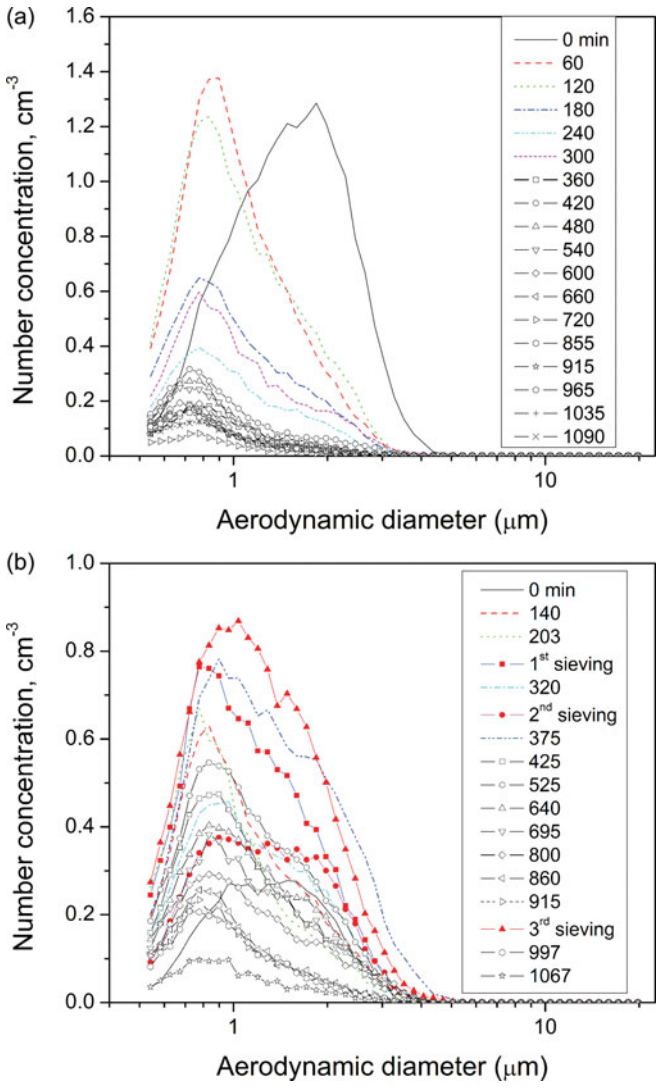


FIG. 10. Size distribution of fibers measured at different times during the 18 h run at 0.1 lpm of aerosol flow rate. (a) Without sieving and (b) with sieving. (Color figure available online.)

TABLE 1
A list of combinations of control parameters to obtain specific aerosol fibers using a vortex shaker for the material tested in this study

| Combination of control parameters | Number concentration for plateau region ($cm^{-3}$) | Fiber size or length |
|---|---|---|
| Batch amount 0.1 $\sim$ 0.5 g, dry air, $Q = 1.5$ lpm, no preshaking | 200 $\sim$ 1000 during the first 10 min (with a dilution ratio of 3.3) | — |
| Batch amount 0.5 $\sim$ 1.0 g, dry air, $Q = 1.5$ lpm, no preshaking | 1000 $\sim$ 3000 during the first 10 min (with a dilution ratio of 3.3) | — |
| Preshaking, dry air, $Q = 1.5$ lpm | — | Generation of larger fibers $> \sim 5$ $\mu$m in aerodynamic diameter |
| Preshaking, humid air (RH = 90%), $Q = 1.5$ lpm | — | Generation of smaller fibers $< \sim 1$ $\mu$m in aerodynamic diameter |
| Dry air, $Q = 0.1$ lpm | — | Generation of smaller fibers $< \sim 4$ $\mu$m in aerodynamic diameter and $L_{50} \sim 2.5$ $\mu$m |
| Dry air, $Q = 0.3 \sim 2.5$ lpm | — | Generation of longer fibers $> L_{50} \sim 10$ $\mu$m; A physical length distribution is similar to that of the batch powder |
| Dry air, $Q = 0.1$ l pm, run a vortex shaker for at least 10 h without sieving | — | Generation of longer fibers $> L_{50} \sim 25$ $\mu$m for leftover in the tube |
| Dry air, $Q = 0.1$ l pm, run a vortex shaker for at least 10 h with sieving | — | Generation of longer fibers $> L_{50} \sim 35$ $\mu$m for leftover in the tube |
| Dry air, $Q = 0.1$ l pm, run a vortex shaker for at least 10 h with 5 sieving and take what is retained on the sieve | — | Generation of much longer fibers $> L_{50} \sim 55$ $\mu$m for leftover on the sieve |



## 5. CONCLUSIONS

A vortex-tube shaking method was characterized with glass fibers to understand its aerosol generation characteristics. Total aerosol concentrations and aerodynamic size distributions were measured for the following different operating conditions: initial batch amounts of glass fibers in the vortex tube, powder preparation (i.e., preshaking), humidity, and rate of airflow. The quality of the aerosol, and its time dependence, were found to depend on all of the above operating parameters.

In summary, we found the following key conclusions:

1. The total fiber number concentration of the aerosol exhibited a characteristic time dependence: the concentration was stable for about $t \sim 10$ min but then precipitously decreased.
2. The magnitude of the concentration plateau increased with powder batch size; the duration of the concentration plateau also increased with powder batch size.
3. The concentration decay, following the concentration plateau, is qualitatively similar for the different batch sizes.
4. The aerodynamic size distribution also evolved with time, with a depletion from the aerosol of the longer fibers over a $\tau \sim$ min timescale.
5. Preshaking the powder enhances the initial aerosol concentration; it also enhances the initial weight in the aerodynamic size distribution at the larger aerodynamic diameters; however, after about $t \sim 3$ min ($\sim$100 exchange volumes) the effects of preshaking disappear.
6. Raising the humidity, from dry air to RH $\sim$ 90%, increased the initial number concentration by a factor of 5; it also slightly reduced the modal diameter in the aerodynamic size distribution.
7. Reducing the aerosol flow reduces the ability to aerosolize the larger fibers. This effect is seen both in the aerodynamic size distribution and in the physical length of the aerosolized fibers.
8. Over long times, $t > 1$ h, the vortex shaker preferentially aerosolizes the longer fibers. This long time depletion of the short fibers from the aerosol is opposite to the intermediate time ($t \sim 10$ min) depletion of the long fibers from the aerosol. This long time effect can be minimized by periodically interrupting the vortex shaking and sieving the residual powder (presumably, breaking up entangled aggregates).

Some recommendations for the use of the vortex shaking method are summarized in the following Table 1.

As a final remark, the complicated time dependences, and the dependence of the aerosol quality (e.g., concentration and aerodynamic size distribution) on a variety of control parameters, indicate that great care should be exercised to monitor the consistency and stability of aerosols generated with the vortex shaker. Also, more work needs to be done for different types of fiber materials in the future to add more data on characterization

of the vortex-shaking method to the limited body of knowledge on the capability of the vortex-shaking method.

## REFERENCES


Baron, P. A., Deye, G. J., Chen, B. T., Schwegler-Berry, D. E., Shvedova, A. A., and Castranova, V. (2008). Aerosolization of Single-Walled Carbon Nanotubes for an Inhalation Study. *Inhal. Toxicol*., 20:751–760.

Donaldson, K., and Poland, C. A. (2009). Nanotoxicology: New Insights into Nanotubes. *Nat. Nanotechnol*., 4:708–710.

ISO. (2012) Nanomaterials—Quantification of Nano-Object Release from Powders by Generation of Aerosols. ISO draft technical specification (draft, as of 2012–02–19) ISO TC 229/SC-N (ISO/PDTS 12025).

Jenkins, J. T., and Yoon, D. K. (2002). Segregation in Binary Mixtures under Gravity. *Phys. Rev. Lett*., 88:194301–194304.

Kim, S. C., Chen, D. R., Qi, C., Gelein, R. M., Finkelstein, J. N., Elder, A., et al. (2010). A Nanoparticle Dispersion Method for In Vitro and In Vivo Nanotoxicity Study. *Nanotoxicology*, 4:42–51.

Kisin, E. R., Murray, A. R., Sargent, L., Lowry, D., Chirila, M., Siegrist, K. J., et al. (2011). Genotoxicity of Carbon Nanofibers: Are They Potentially More or Less Dangerous than Carbon Nanotubes or Asbestos? *Toxicol. Appl. Pharm*., 252:1–10.

Knight, J. B., Ehrichs, E. E., Kuperman, V. Y., Flint, J. K., Jaeger, H. M., and Nagel, S. R. (1996). Experimental Study of Granular Convection. *Phys. Rev. E*., 54: 5726–5738.

Knight, J. B., Jaeger, H. M., and Nagel, S. (1993). Vibration-Induced Size Separation in Granular Media: The Convection Connection. *Phys. Rev. Lett*., 70:3728–3731.

Kohyama, N., Tanaka, I., Tomita, M., Kudo, M., and Shinohara, Y. (1997). Preparation and Characteristics of Standard Reference Samples of Fibrous Minerals for Biological Experiments. *Industrial Health*, 35:415–432.

Ku, B. K., Deye, G., and Turkevich, L. A. (2012). Characteristics of a Vortex Shaking Method for Producing Airborne Glass Fibers for Toxicology Studies, in *Nanotechnology 2012: Biosensors, Instruments, Medical, Environment and Energy,* (NSTI-Nanotech 2012, Nano Science and Technology Institute, 2012). Vol 3, CRC Press, Boca Raton, FL, pp. 358–360.

Ku, B. K., Deye, G., and Turkevich, L. A. (2013). Efficacy of Screens in Removing Long Fibers from an Aerosol Stream—Sample Preparation Technique for Toxicology Studies. *Inhalation Toxicology*.

Ku, B. K., Emery, M. S., Maynard, A. D., Stolzenburg, M. R., and McMurry, P. H. (2006). In situ Structure Characterization of Airborne Carbon Nanofibres by a Tandem Mobility-Mass Analysis. *Nanotechnology*, 17:3613–3621.

Ku, B. K., and Kulkarni, P. (2009). Morphology of Single-Wall Carbon Nanotube Aggregates Generated by Electrospray of Aqueous Suspensions. *J. Nanopart. Res*., 11:1393–1403.

Maynard, A. D., Baron, P. A., Foley, M., Shvedova, A. A., Kisin, E. R., and Castranova, V. (2004). Exposure to Carbon Nanotube Materials I: Aerosol Release during the Handling of Unrefined Single-Walled Carbon Nanotube Material. *J. Tox. Environ. Health A*, 67(1):87–107.

Maynard, A. D., Ku, B. K., Emery, M., Stolzenburg, M., and McMurry, P. (2007). Measuring Particle Size-dependent Physicochemical Structure in Airborne Single Walled Carbon Nanotube Agglomerates. *J. Nanoparticle Res*., 9:85–92.

McKinney, W., Chen, B., and Frazer, D. (2009). Computer Controlled Multi-Walled Carbon Nanotube Inhalation Exposure System. *Inhal. Toxicol*., 21:1053–1061.

Moebius, M. E., Lauderdale, B. E., Nagel, S. R., and Jaeger, H. M. (2001). Size Separation of Granular Particles. *Nature*, 414:270.

Ogura, I., Sakurai, H., and Gamo, M. (2009). Dustiness Testing of Engineered Nanomaterials. *J. Phys.: Conf. Ser.*, 170:012003. doi:10.1088/1742-6596/170/1/012003, 4 p.

Poland, C. A., Duffin, R., Kinloch, I., Maynard, A., Wallace, W. A., Seaton, A., et al. (2008). Carbon Nanotubes Introduced into the Abdominal Cavity of Mice Show Asbestos-like Pathogenicity in a Pilot Study. *Nat. Nanotechnol*., 3:423–428.

Rosato, A., Strandburg, K., Prinz, F., and Swendsen, R. (1987). Why the Brazil Nuts are on Top: Size Segregation of Particulate Matter by Shaking. *Phys. Rev. Lett*., 58:1038.

Spurny, K. R. (1980). Fiber Generation and Length Classification, in *Generation of Aerosols and Facilities for Exposure Experiments*, K. Willeke, ed., Ann Arbor Science Publishers, Ann Arbor, MI, pp. 257–298.

Zeidler-Erdely, P. C., Calhoun, W. J., Ameredes, B. T., Clark, M. P., Deye, G. J., Baron, P., et al. (2006). In Vitro Cytotoxicity of Manville Code 100 Glass Fibers: Effect of Fiber Length on Human Alveolar Macrophages. *Particle Fibre Toxicol*., 3, 7 p.


## APPENDIX: LONG FIBER ENTANGLEMENT

We attempted to verify whether long fiber entanglement is actually occurring in the residual powder as the vortex shaker is run. Gentle sieving, where we let pass through the sieve only that loose material which would penetrate on its own, and where the larger aggregated material is caught on the screen, might allow us to determine if there is a difference in size distribution between entangled and loose fibers. For this experiment, we ran the vortex shaker, as before, at $Q = 0.1$ lpm, for 10 h, stopping to aggressively sieve the residual material in the tube every 2 h. After the final 10 h, we gently sieved the material left in the tube and separated what was retained on the sieve from what penetrated through the sieve. The fiber length distributions of these two fractions are shown in Figure A1. The fiber material that penetrated through the sieve was found to have a length distribution similar to that of the original powder; however, the material captured on the sieve consisted of very long fibers, with a 50% cut-off length $L_{50} \sim 55$ $\mu$m (recall $L_{50} \sim 15$ $\mu$m for the original powder). It may be possible to exploit this effect so as to obtain an enriched sample of longer fibers. This scheme is under current investigation.

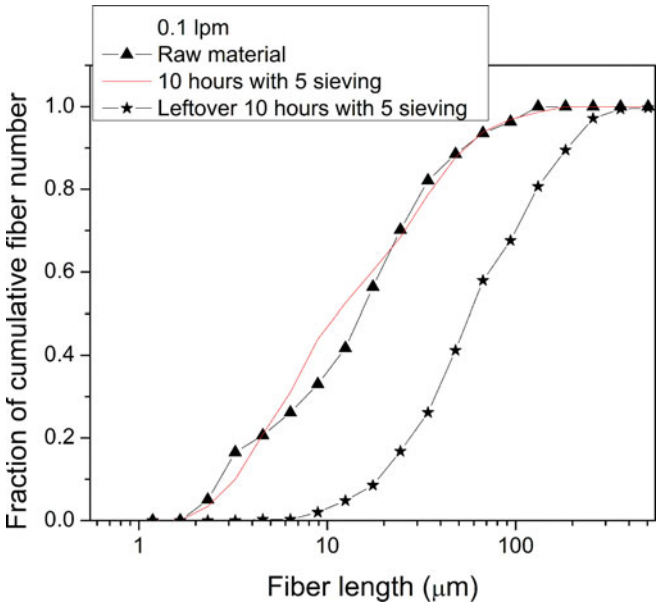


FIG. A1. Fraction of cumulative fiber number vs. fiber length for what was left on the sieve and what penetrated through the sieve for 10 h run with sieving. (Color figure available online.)